Dynein and kinesin regulate stress-granule and P-body dynamics

Mariela Loschi[1,2], Claudia C. Leishman[1], Neda Berardone[1] and Graciela L. Boccaccio[1,2,*]

[1]Instituto Leloir, Avenida Patricias Argentinas 435, C1405BWE-Buenos Aires, Argentina
[2]Facultad de Ciencias Exactas y Naturales, University of Buenos Aires and IIBBA-CONICET, C1405BWE-Buenos Aires, Argentina
*Author for correspondence (gboccaccio@leloir.org.ar)

Journal of Cell Science

Summary

Stress granules (SGs) and P-bodies (PBs) are related cytoplasmic structures harboring silenced mRNAs. SGs assemble transiently upon cellular stress, whereas PBs are constitutive and are further induced by stress. Both foci are highly dynamic, with messenger ribonucleoproteins (mRNPs) and proteins rapidly shuttling in and out. Here, we show that impairment of retrograde transport by knockdown of mammalian dynein heavy chain 1 (DHC1) or bicaudal D1 (BicD1) inhibits SG formation and PB growth upon stress, without affecting protein-synthesis blockage. Conversely, impairment of anterograde transport by knockdown of kinesin-1 heavy chain (KIF5B) or kinesin light chain 1 (KLC1) delayed SG dissolution. Strikingly, SG dissolution is not required to restore translation. Simultaneous knockdown of dynein and kinesin reverted the effect of single knockdowns on both SGs and PBs, suggesting that a balance between opposing movements driven by these molecular motors governs foci formation and dissolution. Finally, we found that regulation of SG dynamics by dynein and kinesin is conserved in *Drosophila*.

Supplementary material available online at
http://jcs.biologists.org/cgi/content/full/122/21/3973/DC1

Key words: Stress granule, P-body, Kinesin, Dynein, Bicaudal

Introduction

Stress granules (SGs) and processing bodies (PBs) are related cytoplasmic silencing foci that harbor silenced messenger ribonucleoproteins (mRNPs). The formation of SGs is triggered by stress-induced phosphorylation of the eukaryotic initiation factor 2α (eIF2α) and by several stimuli that provoke the accumulation of abortive translation-initiation complexes, including pharmacological inhibition of initiation, overexpression of specific translational repressors and the presence of inosine-modified double-stranded RNA (Thomas et al., 2005; Scadden, 2007; Mazroui et al., 2007) (reviewed by Anderson and Kedersha, 2006; Anderson and Kedersha, 2008). SGs contain polyadenylated mRNAs, polyadenylated RNA-binding protein (PABP), initiation factors, small ribosome subunits and a number of RNA-binding proteins. They have been implicated in reprogramming mRNA translation and decay upon stress (Mazroui et al., 2007) (reviewed by Anderson and Kedersha, 2006; Anderson and Kedersha, 2008), and have also been proposed to regulate subcellular localization of key modulators of cell death and proliferation, thus contributing to cell survival (Lin et al., 2007; Stöhr et al., 2007; Yu et al., 2007; Kim et al., 2007; Eisinger-Mathason et al., 2008; Arimoto et al., 2008). The molecular mechanisms underlying their formation have begun to be unveiled. SG assembly is mediated by self-aggregation of specific RNA-binding proteins, namely the T-cell intracellular antigen (TIA1), TIA1-related protein (TIAR) and RasGAP-associated endoribonuclease (G3BP), among others (Tourrière et al., 2003; Anderson and Kedersha, 2006; Anderson and Kedersha, 2008). It has been reported recently that *O*-glycosylation of several proteins contributes to SG as well to PB assembly (Ohn et al., 2008). SGs are transient; their disassembly relies at least partially on HSP70-dependent disaggregation and involves regulated phosphorylation of key protein components (Tourrière et al., 2003;

Mazroui et al., 2007; Tsai et al., 2008) (reviewed by Anderson and Kedersha, 2006; Anderson and Kedersha, 2008).

Whereas SGs contain polyadenylated mRNAs, PBs contain mostly deadenylated repressed mRNAs, as well as several proteins involved in mRNA decapping and decay; unlike SGs, PBs do not contain initiation factors or ribosome subunits (Brengues et al., 2005; Fenger-Grøn et al., 2005) (reviewed by Parker and Sheth, 2007; Eulalio et al., 2007a; Franks and Lykke Andersen, 2008). Similar to SGs, PBs assemble by self-aggregation of specific proteins present in silenced mRNP (reviewed by Franks and Lykke-Andersen, 2008). PBs are present in resting cells and they are further induced upon stress. SGs grow in close contact with PBs, suggesting that an active flow of mRNAs and proteins occurs between the two types of foci (reviewed by Anderson and Kedersha, 2008; Ohn et al., 2008; Mollet et al., 2008; Thomas et al., 2009). Both PBs and SGs are in equilibrium with translating polysomes. The foci dissolve with distinct kinetics when polysomes are pharmacologically stabilized (Brengues et al., 2005; Eulalio et al., 2007b; Kedersha et al., 2005; Sivan et al., 2007) (reviewed by Anderson and Kedersha, 2008; Franks and Lykke-Andersen, 2008). The equilibrium between SGs and polysomes is regulated by Staufen 1, a double-stranded RNA-binding protein that is present in both structures and that apparently stabilizes polysomes (Thomas et al., 2009). SGs and PBs are highly dynamic, and fluorescence recovery after photobleaching (FRAP) analysis has revealed a rapid exchange of mRNAs and proteins with the cytosol (Kedersha et al., 2005; Leung et al., 2006; Aizer et al., 2008; Mollet et al., 2008) (reviewed by Anderson and Kedersha, 2006; Anderson and Kedersha, 2008; Franks and Lykke-Andersen, 2008), thus suggesting that an active transport in and out of the foci, presumably mediated by molecular motors, takes place.

In this work, we explored the role of retrograde and anterograde motors in the regulation of silencing foci formation. Molecular

strategies targeting specific mammalian motor and adaptor subunits led us to the identification of dynein heavy chain 1 (DHC1) and the dynein adaptor molecule bicaudal D1 (BicD1) as key elements for SG assembly. We found that dynein-dependent aggregation of mRNPs is conserved in *Drosophila* and is counteracted by kinesin-driven dispersion, specifically the motor subunit kinesin 1b (KIF5B) and the kinesin light chain subunit 1 (KLC1). We found that PB growth upon stress similarly depends on dynein, and this is antagonized by kinesin. SG formation is not required for global translational silencing and, remarkably, SG dissolution is not required for recovery of protein synthesis, strongly suggesting that mRNAs stored in SGs contribute poorly to restore translation.

Results

Retrograde transport mediated by DHC1 and BicD1 is required for SG formation

We began by evaluating the timecourse of SG formation by monitoring the subcellular distribution of the key SG components eukaryotic initiation factor-η (eIF3η), TIA1 and TIAR in mammalian cell lines exposed to arsenite, a known inducer of oxidative stress (Kedersha et al., 2000; Thomas et al., 2005; Mollet et al., 2008) (reviewed by Anderson and Kedersha, 2006; Anderson and Kedersha, 2008) (supplementary material Fig. S1). We found that, 15 minutes after stress induction, the uniform cytoplasmic staining for eIF3η changed to a punctate pattern. As reported previously, we found that TIA1 and TIAR have a nuclear localization under resting conditions, and that, shortly after stress induction, numerous small aggregates containing TIA1, TIAR and eIF3η begin to form in the cytoplasm (supplementary material Fig. S1A,B) (reviewed by Anderson and Kedersha, 2006; Anderson and Kedersha, 2008; Thomas et al., 2009). Soon afterwards, these particles collapsed into larger granules (supplementary material Fig. S1A,B, 30 minutes), so that, at the peak of the response, fewer and bigger SGs were observed (supplementary material Fig. S1A,B, 60 minutes). Thereafter, 120 minutes after stress induction, the foci began to dissolve synchronously (supplementary material Fig. S1B) and completely vanished 1 hour later. A similar timecourse, with the time of maximal SG formation at around 2 hours and a slower dissolution phase, was observed upon endoplasmic reticulum (ER)-stress induction by thapsigargin (see below). The apparent redistribution of the translational apparatus upon stress induction was not accompanied by a general remodeling of subcellular organization, as judged by the normal distribution shown by the Golgi, the ER and the microtubule-organizing center (MTOC) (supplementary material Fig. S1C), suggesting a selective subcellular transport of SG components.

It is known that the retrograde motor dynein and the anterograde motor kinesin mediate cytoplasmic transport of RNPs in several cell types and organisms (Palacios and St Johnston, 2002; Deacon et al., 2003; Hughes et al., 2004; Ling et al., 2004; Bullock et al., 2006; Kanai et al., 2004; Delanoue et al., 2007; Dictenberg et al., 2008; Horne-Badovinac and Bilder, 2008; Li et al., 2008). To investigate the participation of dynein in SG dynamics, we first analyzed the presence of dynein subunits in SGs by immunofluorescence performed in fixed or live-extracted COS-7, NIH3T3, HeLa, BHK or primary cells (Fig. 1A-C, supplementary material Fig. S2A, and M.L. and G.L.B., unpublished observations). We found that SGs contain a significant amount of dynein intermediate chain (DIC) and dynein heavy chain (DHC) – the motor subunit carrying the ATPase activity – as judged by a strong colocalization of these molecules with either PABP (a surrogate

marker for polyadenylated RNA) (Fig. 1A,B), with the SG core component TIAR (Fig. 1C), with eIF3η (supplementary material Fig. S2A) or with the SG marker Staufen 1 (M.L. and G.L.B., unpublished observations). Next, we analyzed the effect of overexpressing p50 (also known as dynamitin), a subunit of the dynactin adaptor complex that is known to titrate dynein motors, thus acting as a dominant negative (Deacon et al., 2003; Burakov et al., 2008). As shown in Fig. 1D and E, arsenite-induced SG formation was dramatically impaired upon transfection of p50. The number of cells forming SGs, as assessed by TIA1, TIAR or Staufen-1 staining, was reduced throughout the entire response as compared with non-transfected cells or cells transfected with control constructs (Fig. 1D,E; M.L. and G.L.B., unpublished observations). The above experiments indicate that disruption of dynein activity impairs SG formation and agree with previous observations based on pharmacological approaches (Kwon et al., 2007; Tsai et al., 2009). p50 is known to affect dynein-dependent transport and, thus, we speculate that p50 overexpression impairs SG formation after global translation silencing and concomitant polysome disassembly. By contrast, we recently reported that overexpression of Staufen 1 impairs SG formation by stabilizing polysomes (Thomas et al., 2009). Here, we analyzed whether the blockage of SG formation upon overexpression of p50 or Staufen 1 is affected by enhancing polysome disruption with puromycin. We found that puromycin had no effect on the p50-mediated inhibition of SG formation, whereas it partially released the Staufen-1-mediated blockage (supplementary material Fig. S2B). These observations support the notion that p50 overexpression affects a step downstream of polysome disassembly.

Next, we further analyzed which particular cytoplasmic DHC subunit, DHC1 or DHC2, participates in SG assembly. Dramatic impairment of SG formation was observed upon siRNA-mediated silencing of DHC1, but not of DHC2, upon exposure to the ER-stress inducer thapsigargin (Fig. 1F,G) or to arsenite (Fig. 1H,I). In all cases, SGs were either completely absent or dramatically reduced in number and size in siDHC1-treated cells (Fig. 1G,I). No synergistic effect was observed upon simultaneous treatment with siDHC2 and, as expected, the inhibitory effect was lower when the concentration of siDHC1 was reduced from 100 to 50 nM (see below). The inhibitory effect was verified with two independent siRNA sequences and was observed at all time points upon exposure to several stressors (Fig. 1F-I; supplementary material Fig. S2C-E and Fig. S3). Finally, the effect of siDHC1 was confirmed by visualizing the distribution of eIF3η (supplementary material Fig. S2F,G). Effective dynein knockdown was verified as shown in supplementary material Fig. S4. Altogether, these results indicate a role for DHC1 in SG aggregation, which is in accordance with the requirement of dynein light chain (DLC) 2A reported recently in neurons (Tsai et al., 2009). The effect is likely to be direct on the transport and/or anchorage of mRNA and proteins, given the remarkable colocalization of both DHC and DIC (Fig. 1A-C and supplementary material Fig. S2A), as well as that of DLC2A (Tsai et al., 2009), with SG markers.

Molecular motors require adaptors for their interaction with RNPs. Bicaudal D is an evolutionarily conserved protein with a well-documented role as dynein adaptor for the transport of several membranous organelles (Hoogenraad et al., 2001; Matanis et al., 2002; Fumoto et al., 2006). It is also known that *Drosophila* bicaudal D is involved in mRNP transport in the oocyte and embryo (Hughes et al., 2004; Delanoue et al., 2007; Bullock et al., 2006). The mammalian genome includes two homologs, BicD1 and BicD2, that
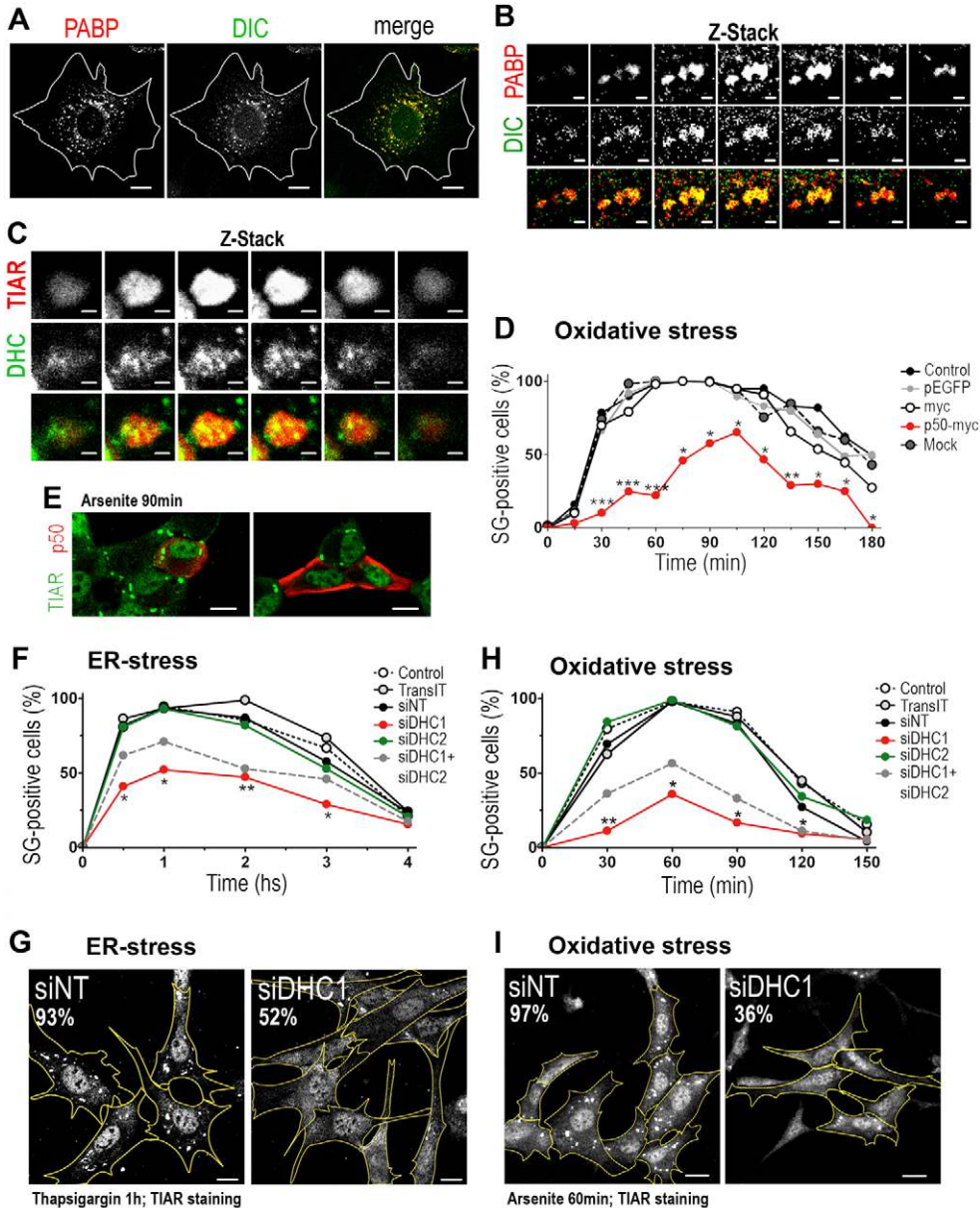
Fig. 1. Dynein mediates SG formation. (A-C) DIC and DHC are detected in SGs. (B,C) Single SGs were analyzed by confocal slicing (0.4-µm slices). (A,B) COS-7 cells were exposed to arsenite and SGs were visualized in permeabilized cells by staining for PABP. All SGs contain DIC (A) and confocal slicing of a representative SG from panel A showed strict colocalization of DIC with PABP (B). (C) A representative SG identified by TIAR staining in permeabilized NIH3T3 cells was analyzed by confocal slicing, showing the presence of DHC. (D) Overexpression of the dynactin subunit p50 inhibits SG formation. NIH3T3 cells were transfected with the indicated plasmids and exposed to 0.5 mM arsenite. SGs were visualized by staining for the SG marker Staufen 1 at the indicated times after stimulation. Transfection of p50 impaired SG formation, whereas no significant differences were observed among mock-transfected, non-transfected, EGFP-expressing or Myc-tag-expressing cells (see Materials and Methods for cell scoring; *$P<0.05$; **$P<0.01$; ***$P<0.001$). A representative experiment out of three is shown. (E) SGs formed normally in lower-expressing cells (left panel) and were absent in most cells overexpressing p50 (right panel). (F-I) DHC1 knockdown impairs SG formation. NIH3T3 cells were treated with the indicated siRNAs (see Materials and Methods) and exposed to 5 µM thapsigargin (F,G) or 0.5 mM arsenite (H,I). SGs were identified by TIAR. A representative experiment out of three is shown in each case. Effective DHC1 knockdown, and microtubule integrity upon siDHC1 treatment were confirmed (supplementary material Fig. S4A,C). (G,I) TIAR appeared cytosolic, and SGs were absent or reduced in number and size in most siDHC1-treated cells (see also supplementary material Fig. S3). Scale bars: 10 µm (A,E,G,I); 1 µm (B,C).

contain several almost identical coiled-coil regions, and a less conserved C-terminal domain, which is believed to interact with the cargo. The relevance of mammalian BicD1 and BicD2 in mRNP transport, or in the formation of cytoplasmic aggregates, has not been addressed so far, so we analyzed whether these adaptor molecules are required for SG formation. As above, siRNA pools against the target molecules were used. After induction of ER or oxidative stress, we found that cells depleted of BicD1 showed an impairment of SG formation similar to that observed upon DHC1 knockdown (Fig. 2A-D and supplementary material Fig. S3). As expected, a synergistic effect was observed when BicD1 and DHC1 were simultaneously silenced (Fig. 2C). BicD2 knockdown had no effect on SG assembly upon oxidative or ER stress (Fig. 2A-D and supplementary material Fig. S3). Moreover, when BicD1 and BicD2 were simultaneously silenced, the effect was equivalent to that observed upon BicD1 single knockdown. This indicates that BicD2 does not contribute to SG formation even in the absence of BicD1 (Fig. 2D). Effective knockdown of BicD1 and BicD2 was

confirmed by reverse-transcription PCR (RT-PCR) (supplementary material Fig. S4A) and by monitoring the anchorage of microtubules to the MTOC (Fig. 2E). As expected (Fumoto et al., 2006), no effect on microtubule anchoring was observed when either BicD1 or BicD2 were independently silenced, whereas microtubule detaching was clearly observed upon simultaneous knockdown of BicD1 and BicD2 (Fig. 2E), in contrast to the lack of synergy in the inhibition of SG formation (Fig. 2D). Altogether, the above results indicate that DHC1 and BicD1 mediate SG formation.

In agreement with the requirement of microtubule-dependent motors for SG assembly, we found that microtubule integrity was also required for SG formation. Pharmacological disruption of microtubules by exposure to colchicine or nocodazole led to the formation of smaller and more numerous SGs, which also had anomalous subcellular distribution (supplementary material Fig. S5A, and M.L. and G.L.B., unpublished observations); there were no changes in the proportion of cells that showed foci. Using a similar approach, other authors reported that microtubule
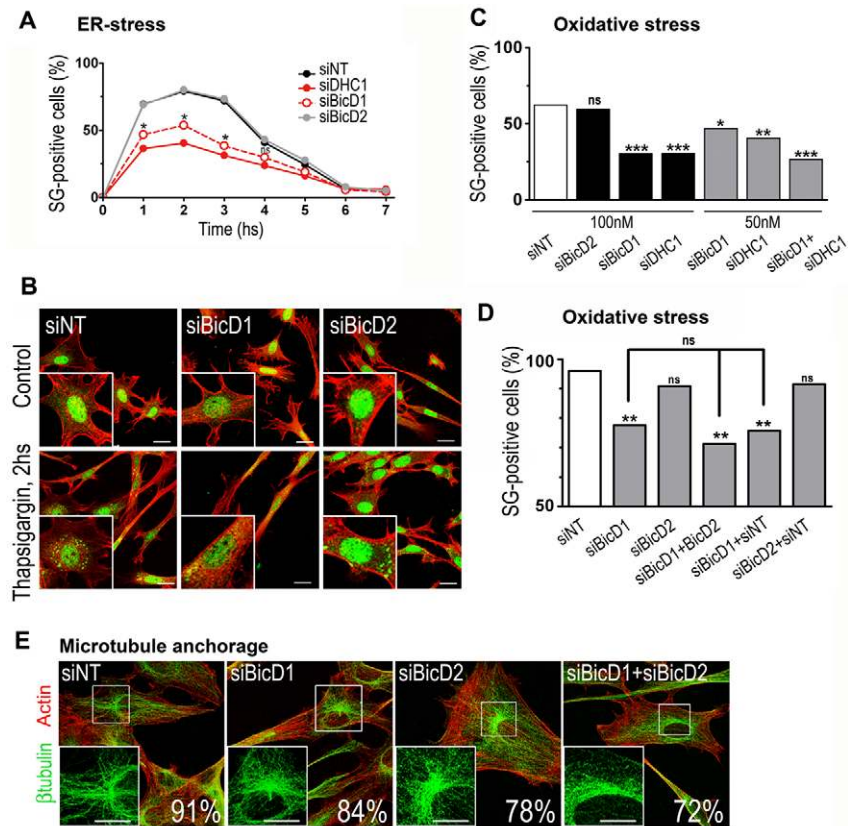
Fig. 2. BicD1 is required for SG assembly. (A-D) NIH3T3 cells were treated with the indicated siRNAs at the indicated concentrations prior to the induction of ER stress (A,B) or oxidative stress (C,D) as indicated in Materials and Methods. SGs were identified by TIAR staining (green), and SG formation was scored as indicated in Materials and Methods. Microfilaments appear red. SG formation was impaired by BicD1 knockdown in both stress models (A-D), whereas siBicD2 has no effect (A,B,D). ns, not significant; *$P<0.05$; **$P<0.01$; ***$P<0.001$. (B) Representative micrographs from the experiment in A. SG formation in siBicD2-treated cells was equivalent to that of siNT-treated cells, whereas SGs were absent or reduced in number and size upon BicD1 depletion. See supplementary material Fig. S3 for representative micrographs upon BicD1 or BicD2 knockdown and oxidative-stress induction. (C) A dose-dependent effect of siDHC1 and siBicD1 was observed, and simultaneous knockdown of DHC1 and BicD1 synergized the inhibition. (D) siBicD2 had no effect on SG formation upon oxidative stress either in the presence or absence of siBicD1. No significant differences were observed between cells treated with siBicD1, siBicD1 + siNT or siBicD1 + siBicD2. (E) Effective knockdown of BicD1 and BicD2 was confirmed by monitoring the anchorage of microtubules (green) to the MTOC. Percentages of the most frequent phenotypes are indicated. Upon treatment with siNT, siBicD1 or siBicD2, most cells showed anchored microtubules, whereas, upon treatment with siBicD1 + siBicD2, 72% of cells showed detached microtubules. Scale bars: 10 µm.

depolymerization dramatically reduced the fraction of cells with SGs (Ivanov et al., 2003; Kwon et al., 2007) and, more recently, Kolobova et al. (Kolobova et al., 2009) showed an effect similar to that reported here. Altogether, these observations support a role of microtubules in SG assembly. We have also analyzed the effect of microfilament disruption in SG formation. In contrast to a previous report that showed a facilitative effect (Ivanov et al., 2003), we found that microfilament depolymerization impaired SG growth, provoking the formation of scattered and highly numerous foci (supplementary material Fig. S5A) without affecting the overall number of cells exhibiting SGs. Our results suggest that, in addition to microtubule-dependent motors, yet-unknown myosins play a role in SG fusion and growth.

The anterograde motor kinesin is required for SG disassembly

Having established that dynein-dependent retrograde transport is required for SG formation, we investigated whether the anterograde motor kinesin is involved in SG dissolution. Mammalian conventional kinesin is a tetrameric molecule composed of two heavy chains (KHC, also known as KIF5 or kinesin 1) and two light chains (KLC) (DeBoer et al., 2008). As above, we analyzed the presence of kinesin subunits in SGs. Three distinct antibodies against distinct KHC epitopes (see Materials and Methods) yielded a positive immunofluorescence signal in SGs induced in COS-7, HeLa, BHK, NIH3T3 or primary cells (Fig. 3A-C, supplementary material Fig. S1B and S5G, and M.L. and G.L.B., unpublished observations). As for dynein, KHC was observed in every SG identified by PABP, TIA1, TIAR or Staufen 1, including the small aggregates that appear shortly after stress induction (Fig. 3A and supplementary material Fig. S1B). In addition, the light subunit was detected in SGs by two distinct antibodies (see Materials and

Methods), in NIH3T3, HeLa, BHK or primary cells (Fig. 3D, supplementary material Fig. S5B-G, and M.L. and G.L.B., unpublished observations). Together, these results indicate that kinesin occurs in SGs. Next, we analyzed the effect of kinesin-subunit knockdown. We found that NIH3T3 cells depleted of the ubiquitous kinesin heavy chain KIF5B and exposed to ER or oxidative stress formed SGs of normal size and number. However, the number of cells with SGs was slightly increased and, remarkably, SG dissolution was delayed by about 2 hours upon ER stress (Fig. 3E,F and supplementary material Fig. S6) and by 30 minutes upon oxidative stress (Fig. 3G) in KIF5B-depleted cells. We also analyzed the effect of knockdown of the ubiquitous kinesin light chains KLC1 and KLC2. Depletion of KLC1 also provoked a prolonged persistence of SGs, paralleling the effect of KIF5B silencing (Fig. 3H and supplementary material Fig. S6), but no effect was observed upon KLC2 knockdown. Altogether, these results indicate that the mammalian kinesin subunits KIF5B and KLC1 are required for SG disassembly.

A balance between kinesin- and dynein-driven transport regulates SG and PB growth

We wondered whether dynein- and kinesin-dependent transport are sequentially activated, accounting for the transient formation of SGs, or whether, alternatively, dynein and kinesin are permanently active, so that their aggregative and dispersing forces compete throughout the formation and dissolution processes. To distinguish between these two possibilities, we performed a double knockdown of the dynein and kinesin motor subunits DHC1 and KIF5B, and exposed the cells to oxidative or ER stress (Fig. 4). We found that the impairment of SG formation upon DHC1 knockdown was reverted by kinesin depletion, suggesting that kinesin is active during
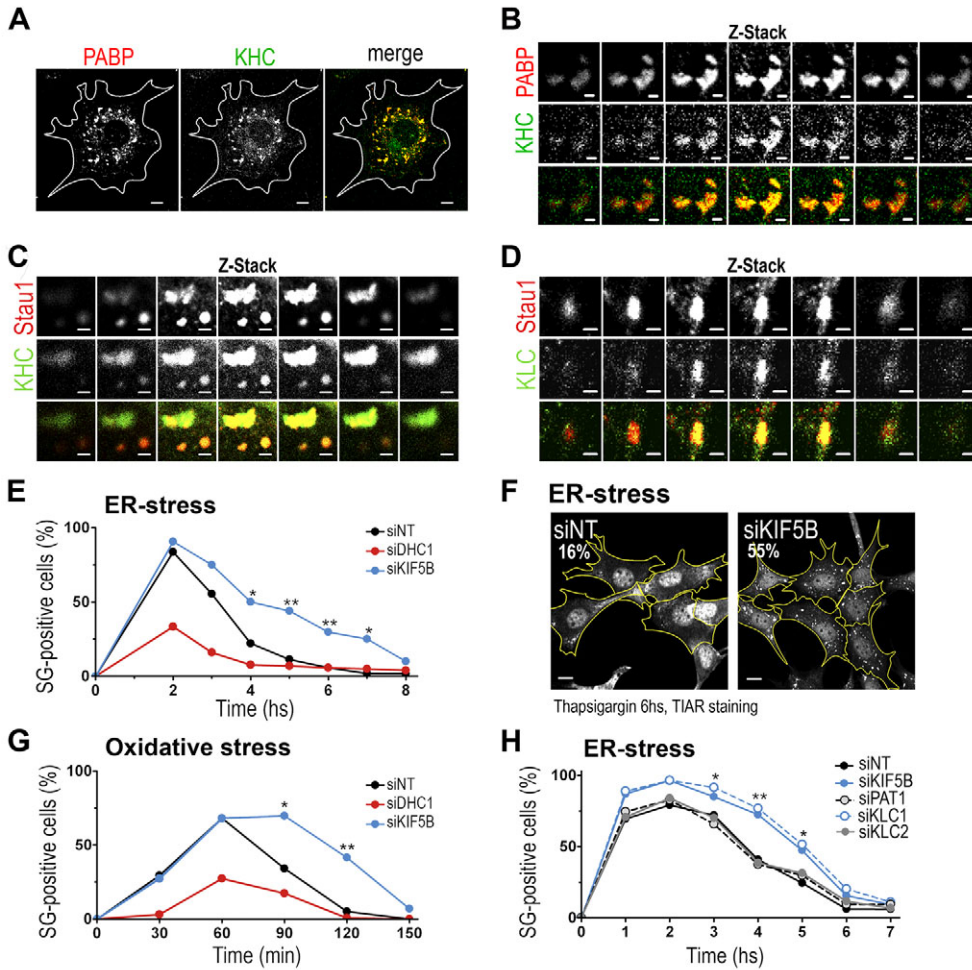
Fig. 3. Kinesin mediates SG disassembly. (A-D) KHC (A-C) and KLC (D) were detected in arsenite-induced SGs with the H2 and L1 antibodies, respectively (see Materials and Methods). (B-D) Single SGs were analyzed by confocal slicing (0.4-μm slices). (A) KHC is recruited to SGs identified by PABP in permeabilized COS-7 cells. (B) Confocal slicing of representative SGs from panel A, showing strict colocalization. (C,D) Representative SGs identified by Staufen-1 staining in Triton-X-100-extracted NIH3T3 cells showing the presence of KHC and KLC. (E-H) NIH3T3 cells were independently treated with siRNAs against *DHC1*, *KIF5B*, *KLC1*, *KLC2* or the partially homologous molecule PAT1 (see Materials and Methods). Effective KIF5B knockdown, and integrity of the microtubule lattice upon siKIF5B treatment were confirmed (supplementary material Fig. S4B-E). ER stress or oxidative stress was induced, and cells were scored as indicated in Materials and Methods. (E,G) SGs disassembled slowly upon KIF5B silencing, whereas dynein knockdown impaired SG formation in both stress models. A representative experiment out of three is shown in each case. SGs were identified by TIAR staining. (F) SGs of normal size and number, but that were significantly more persistent, were observed upon siKIF5B silencing. (H) SGs disassembled slowly upon treatment with siKIF5B or siKLC1, whereas siKLC2 or siPAT1 had no effect. See supplementary material Fig. S6 for representative micrographs of all time points upon thapsigargin treatment. Scale bars: 10 μm (A,F); 1 μm (B-D).

the aggregation phase, thus antagonizing dynein-mediated aggregation (Fig. 4A-C). Conversely, the impairment of SG dissolution provoked by kinesin knockdown was partially compensated by dynein silencing. This indicates that dynein-mediated aggregation opposes kinesin-mediated dispersion during the dissolution phase (Fig. 4A, 6- and 8-hour time points, and Fig. 4B, 90-150 minutes).

Next, we investigated whether knockdown of motor molecules also affects PBs in resting or stress conditions. We simultaneously analyzed SGs and PBs upon treating cells with thapsigargin or arsenite. As reported previously (Mollet et al., 2008; Thomas et al., 2009), we found that SGs form adjacent to apparently pre-existing PBs and, as expected, PB growth was induced by cellular stress. At the time of maximal SG formation, PB size increased from about 0.7 μm in resting conditions up to 1.1-1.5 μm upon oxidative or ER stress (Fig. 4D,E). Next, we investigated the effect on PBs of knocking down dynein or kinesin. We found that neither DHC1 nor KIF5B knockdown under resting conditions affect significantly the number or size of PBs (Fig. 4D,E). The effect of siRNAs targeting these motor molecules was also analyzed upon stress induction. We found that stress-induced growth of PBs was abrogated by silencing of DHC1 in both ER- and oxidative-stress models (Fig. 4D,E). Because PBs and SGs are believed to actively exchange molecules, and mRNAs are sorted from SGs to PBs (Kedersha et al., 2005), we wondered whether inhibition of PB growth was linked to a lack of SGs. To address this issue, the effect on PBs was analyzed in

stressed cells exhibiting SGs or not. We found that silencing of DHC1 affected PB induction independently of the presence of SGs induced either by ER stress (Fig. 4D) or oxidative stress (Fig. 4E and supplementary material Fig. S7A,B). These observations indicate that the defect on PB growth is not due to a reduced flow of material from SGs and therefore suggest that, instead, silenced mRNPs coming from the cytosol directly accumulate into PBs by the action of dynein. The effect of kinesin knockdown was similarly analyzed. We found that PBs are induced to normal or slightly higher levels in siKIF5B-treated cells (Fig. 4D,E and supplementary material Fig. S7A,B). Finally, we analyzed the effect of simultaneous knockdown of DHC1 and KIF5B on PB dynamics. We found that, as for the case of SGs, the inhibition of PB growth upon dynein depletion was reverted by simultaneous silencing of kinesin. In both stress models, PB size in cells that were treated with siDHC1 and siKIF5B was comparable to that of stressed cells treated with a non-relevant siRNA (Fig. 4D). Altogether, these observations suggest that dynein and kinesin exert opposing effects that regulate the assembly of the two types of silencing foci, probably by mediating the transport in and out of silenced mRNPs.

SG dissolution is not required to restore translation
Cellular stress triggers the phosphorylation of eIF2α by specific kinases, thus inducing the formation of SGs (Mazroui et al., 2007) (reviewed by Anderson and Kedersha, 2008). Hence, we investigated whether altered dynamics of silencing foci upon
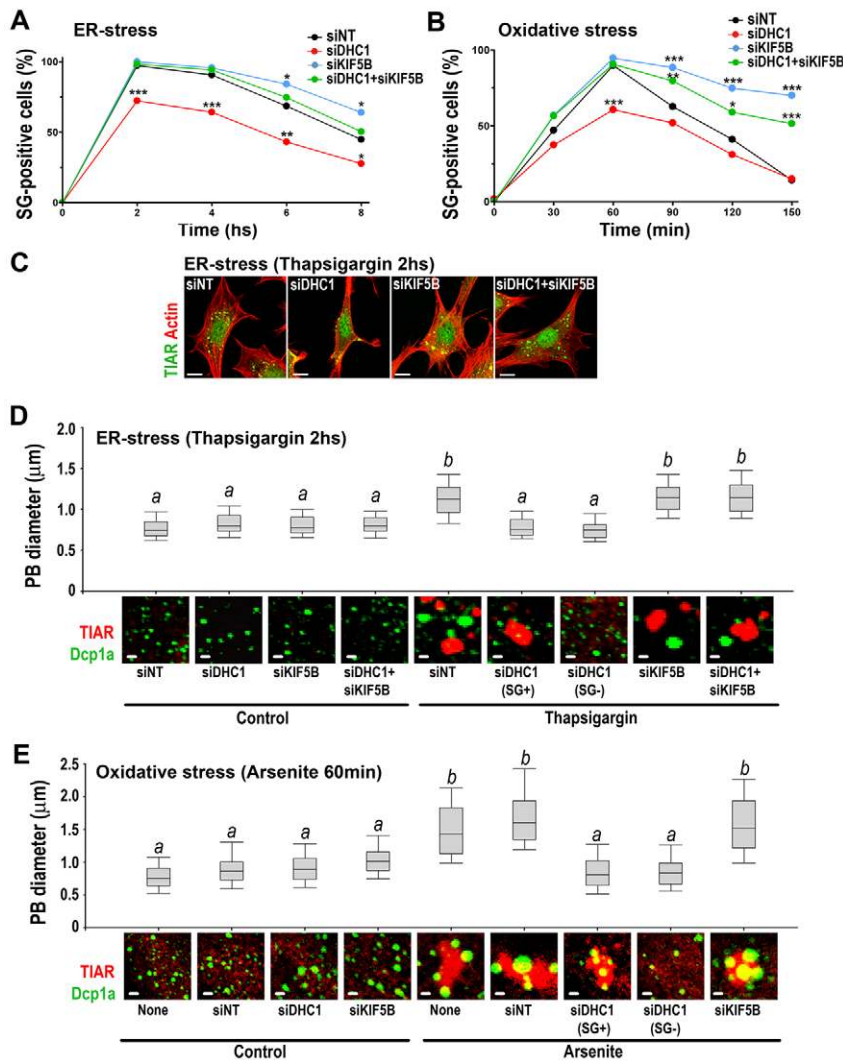
Fig. 4. A balance between dynein and kinesin regulates the formation of silencing foci. DHC1 and KIF5B were simultaneously or independently silenced using the indicated siRNAs (used at 50 nM in A-D, or at 100 nM in E; siNT was used at 100 nM in all cases). Cells were exposed to thapsigargin (A,C,D) or arsenite (B,E), SGs were identified by TIAR staining and cells were scored as in Figs 1-3. The effect of single knockdown of kinesin or dynein on SG formation and dissolution was compensated by simultaneous silencing of the opposite motor (A,B). (C) Representative micrographs from experiment in A, showing SGs that were formed after 2 hours treatment with thapsigargin upon single or double knockdown of the indicated molecules. SGs were absent or reduced in number and size upon DHC1 depletion, whereas no differences were observed upon KIF5B or simultaneous silencing of DHC1 and KIF5B. (D,E) The average diameter of PBs identified by DCP1a staining (green) was measured for more than 300 PBs from 20 cells randomly selected for each treatment. SGs were simultaneously identified by TIAR staining (red). Medias by one-way ANOVA and SNK multiple comparisons post *t*-test indicate significant differences (*P*<0.01) between data groups *a* and *b*. Basal PBs were not affected by siDHC1 at either 50 nM (D) or 100 nM (E), whereas their growth upon ER stress (D) or oxidative stress (E) was impaired. The effect was independent of the presence of SGs and both free PBs as well as those adjacent to SGs were affected. The inhibitory effect on PB growth was compensated by simultaneous silencing of KIF5B. Scale bar: 10 µm (C); 0.5 µm (E,F).

knockdown of molecular motors is linked to altered eIF2α phosphorylation. We found that depletion of dynein or kinesin did not affect the transient phosphorylation of eIF2α upon either ER or oxidative stress (Fig. 5A,B, and M.L. and G.L.B., unpublished observations). Simultaneous knockdown of dynein and kinesin also had no effect (M.L. and G.L.B., unpublished observations). In all cases, eIF2α phosphorylation reached similar maximal levels at the time of maximal SG formation and decayed to basal levels regardless of the presence of SGs. This is consistent with the notion that motor-driven transport of RNPs is downstream of eIF2α phosphorylation. We further investigated whether disruption of SG assembly and PB growth upon dynein knockdown alters the transient translational blockage triggered by stress. We found that a significant reduction of SG formation provoked by DHC1 knockdown (Fig. 5A) had no effect on the inhibition of protein synthesis triggered by oxidative or ER stress (Fig. 5C,D). These results indicate that the presence of microscopically visible SGs is not required for global translational silencing, and that SG formation and PB growth are the consequence of translational silencing and motor-molecule-mediated nucleation.

Next, we analyzed whether SG dissolution is required to restore translation. This was not the case, because we found that, when SGs were forced to last longer upon kinesin knockdown, the recovery of translation that correlates with normal SG dissolution and eIF2α reactivation was not affected (Fig. 5A,C, 4-10 hours). In all cases, we observed that protein synthesis recovered partially, to approximately 50% of basal levels, as previously reported (Mazan-Mamczarz et al., 2006). These observations suggest that mRNAs transiently stored in SGs do not represent a major proportion of the pool of mRNAs that resume translation.

Regulation of SG dynamics by molecular motors is conserved in *Drosophila*

Whereas stress-induced SGs have been described in mammalian and plant cells, and related foci were recently reported in yeast (Buchan et al., 2008) (reviewed by Anderson and Kedersha, 2008), their occurrence in *Drosophila* has not been reported so far. By monitoring the distribution of polyadenylated RNA, we observed that SGs are induced in *Drosophila* S2R+ cells upon oxidative or ER stress (Fig. 6A,B). As in mammalian cells, SGs in *Drosophila* associate to PBs (Fig. 6B) and, as expected for bonafide SGs (Anderson and Kedersha, 2006; Mollet et al., 2008; Ohn et al., 2008), these foci were sensitive to the polysome-stabilizing drug cycloheximide (Fig. 6C). Paralleling the behavior of SGs in mammalian cells, treatment of S2R+ cells with dsRNA against *Drosophila* dynein (DHC64C) impaired their formation (Fig. 6D).
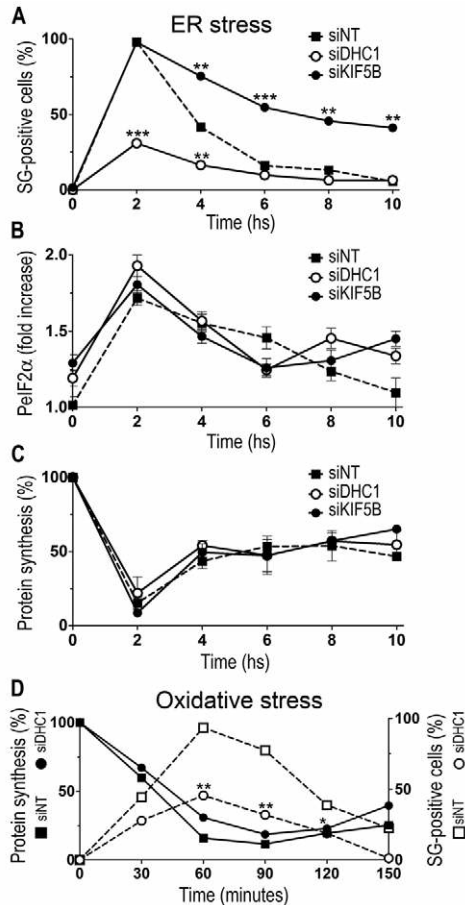
Fig. 5. SG disassembly is not required to restore translation. ER stress (A-C) or oxidative stress (D) was induced in NIH3T3 cells treated with the indicated siRNAs. SGs were identified by TIAR staining. In both stress models, eIF2α phosphorylation (B) was maximal, and protein synthesis (C,D) was minimal at the peak of SG formation (2 hours upon ER stress; 60-90 minutes upon oxidative stress). Thereafter, eIF2α phosphorylation decayed to basal levels, and protein synthesis recovered up to 60% of basal levels. (B) eIF2α phosphorylation was not significantly affected by knockdown of either dynein or kinesin. (C) Translational silencing upon ER stress was not significantly affected after siDHC1 knockdown; protein synthesis was reduced as in control cells to 20% respective of basal levels. By contrast, SG formation was reduced upon siDHC1 knockdown from 98% to 30% (A). Upon KIF5B knockdown, SGs lasted longer, and the recovery of translation between 4 to 10 hours post-stimulus, which correlates with normal SG disassembly (A) and with de-phosphorylation of eIF2α (B), was not affected. (D) Inhibition of protein synthesis upon oxidative stress was not significantly affected by siDHC1. *$P<0.05$; **$P<0.01$; ***$P<0.001$.

Conversely, knockdown of *Drosophila* KHC prolonged the presence of SGs (Fig. 6D).

Discussion

Our findings have revealed a conserved requirement of dynein-mediated transport for SG assembly upon stress exposure. We propose that, following protein-synthesis inhibition, regulated self-assembly of key proteins (Ohn et al., 2008) (reviewed by Anderson and Kedersha, 2008) and an active subcellular transport driven by dynein lead to the formation of SGs harboring abortive initiation complexes (this work) (Kwon et al., 2008; Tsai et al., 2009). The molecular mechanism underlying SG dissolution is less well understood. It is known that SG disassembly depends on the activity

of the chaperone HSP70 that accumulates upon stress induction, and on the phosphorylation of specific proteins present in SGs (Tourrière et al., 2003; Mazroui et al., 2007; Tsai et al., 2008) (reviewed in Anderson and Kedersha, 2006; Anderson and Kedersha, 2008). Our results have revealed that kinesin-dependent anterograde transport mediates SG dissolution in both mammals and *Drosophila* cells (Fig. 6E). Remarkably, we have found that the antagonistic activities of dynein and kinesin apparently compete throughout the assembly and subsequent disassembly of SGs. We have also found that PB growth upon stress depends on the action of dynein, and, as for SGs, the relative activities of dynein and kinesin determine the extent of PB growth upon stress induction. SGs and PBs exchange mRNA and proteins with the cytosol permanently (Kedersha et al., 2005; Leung et al., 2006; Aizer et al., 2008; Mollet et al., 2008) (reviewed in Anderson and Kedersha, 2006; Anderson and Kedersha, 2008; Franks and Lykke-Andersen, 2008), and our results now suggest that dynein and kinesin account for the shuttling of distinct silenced mRNPs in and out of SGs and PBs. Thus, we propose that the integrity of silencing foci depends on a balance between the antagonistic activities of dynein and kinesin, so that a constant delivery of mRNPs mediated by dynein prevents a premature dissolution provoked by the constant release of mRNPs mediated by kinesin (Fig. 6E).

Molecular motors are multi-subunit complexes. By targeting several candidate motor and adaptor subunits, we identified DHC1 and BicD1 as cardinal mediators of SG aggregation, and the kinesin-1 heavy chain KIF5B as well as the light chain KLC1 as mediators of dissolution. The involvement of dynein in the formation of SGs and PBs is reminiscent of the role of this molecular motor in the nucleation of aggresomes, which are cytoplasmic accretions of unfolded polyubiquitylated proteins (reviewed by Kopito et al., 2000). In line with this, it has been recently shown that, similar to aggresomes, SGs contain ubiquitin, and that their assembly requires histone deacetylase 6 (HDAC6), a protein that binds ubiquitin and interacts with the dynein adaptor dynactin (Mazroui et al., 2007; Kwon et al., 2007). Whether the formation of aggresomes and SGs upon stress exposure is somehow coordinated is unknown.

Whereas the retrograde motor dynein has been involved in the formation of protein aggregates and mRNA transport (Kopito, 2000; Palacios and St Johnston, 2002; Deacon et al., 2003; Hughes et al., 2004; Ling et al., 2004; Bullock et al., 2006; Kanai et al., 2004; Delanoue et al., 2007; Dictenberg et al., 2008; Horne-Badovinac and Bilder, 2008; Li et al., 2008), the relevance of the mammalian adaptors BicD1 and BicD2 in these processes has not been addressed. We found that BicD1, but not BicD2, is required for SG assembly. The *Drosophila* genome contains only one bicaudal gene, which was shown to participate in mRNP transport in several cellular contexts (Hughes et al., 2004; Delanoue et al., 2007; Bullock et al., 2006), as well as one *KLC* gene, which has not been shown to be involved in mRNP transport. Thus, it seems likely that these molecules contribute to SG dynamics, as do their mammalian homologs.

The relationship between translational silencing upon stress exposure and the formation of silencing foci is a relevant issue. The fact that SGs harbor abortive translation-initiation complexes as well as initiation factors released from mRNAs has led to the speculation that SGs help to silence global protein translation (Scaden, 2007; Lin et al., 2007) (reviewed by Anderson and Kedersha, 2008). However, it has been recently shown that inhibition of SG formation by impairment of *O*-glycosylation has no effect on polysome disruption upon oxidative stress in mammalian cells (Ohn et al.,
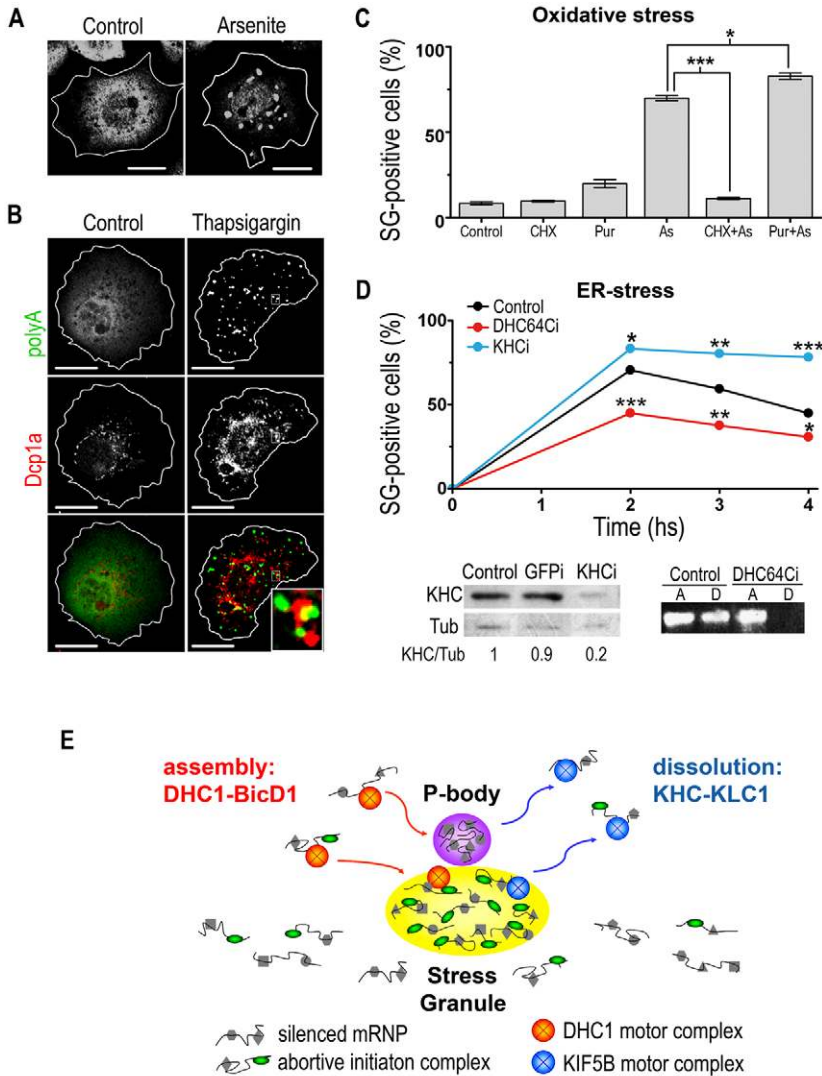
Fig. 6. The function of dynein and kinesin is conserved in *Drosophila*. *Drosophila* S2R+ cells were exposed to 0.5 mM arsenite (A) or to 0.5 µM thapsigargin (B). SGs were identified by staining polyadenylated RNA, and PBs by staining DCP1a. Scale bars: 10 µm. (C) Cells were exposed to 0.5 mM arsenite (As) in the presence or absence of cycloheximide (CHX) or puromycin (Pur). Polysome stabilization by cycloheximide impaired SG formation, whereas polysome disruption by puromycin had a moderate enhancing effect. (D) Cells were treated with the indicated dsRNA as indicated in Materials and Methods (GFP, green fluorescent protein) and exposed to arsenite during the indicated times. *Drosophila* DHC (DHC64C) knockdown impairs SG formation, whereas KHC knockdown prolonged their presence. Effective KHC knockdown was confirmed by western blot (bottom left); KHC signal intensity relative to that of tubulin (Tub) is indicated. Effective DHC64C knockdown was confirmed by RT-PCR analysis (bottom right). 'A', actin; 'D', DHC64C. (E) A model for a role of the subcellular transport system in SG and PB assembly. Protein-synthesis inhibition by cellular stress or pharmacological inhibition of 60S joining provokes the formation of abortive translation-initiation complexes, which are not present in PBs, and other silenced mRNPs. We propose that dynein transports abortive translation-initiation complexes and distinct mRNPs to growing SGs and PBs. In addition, given that depletion of yeast or mammalian PBs might impair SG formation (Buchan et al., 2008; Ohn et al., 2008; Thomas et al., 2009), it cannot be ruled out that inhibition of PB growth upon dynein knockdown contributes at least partially to the inhibition of SG formation. We also propose that delivery of silenced mRNPs from the cytosol to silencing foci is antagonized by a transport mediated by KHC and KLC1, which mediates foci dissolution. Given that SG disassembly is not required to restore global protein translation, we propose that a large proportion of silenced mRNPs remains outside microscopically visible foci. The possibility that specific mRNAs are sequestered in the SG compartment remains open (see Discussion).

2008). In line with this, yeast strains defective in SG formation can still block protein synthesis upon stress induced by glucose deprivation (Buchan et al., 2008). Similarly, it is now accepted that recruitment of mRNPs to PBs is not a requirement but a consequence of translational repression (Leung et al., 2006; Eulalio et al., 2007b) (reviewed by Franks and Lykke-Andersen, 2008). In agreement with these reports, our data support the notion that microscopically visible SGs are not required for translational silencing upon stress. The contribution of submicroscopic structures to translational silencing remains to be investigated. Our observations suggest that SG formation and PB growth result from the release of mRNAs from polysomes after eIF2α phosphorylation.

Because translation is not possible in the SG compartment, it seems reasonable that mRNPs need to be released from the silencing foci for the cell to resume translation after eIF2α reactivation. Our results indicate that this is not the case. We found that SG dissolution and concomitant mRNP release is not required to restore general protein translation, implying that most mRNAs destined to resume translation are not stored in SGs. We have not investigated whether prolonged presence of SGs upon kinesin knockdown affects the profile of mRNAs that are translated upon eIF2α reactivation and, therefore, the possibility that SGs sequester specific mRNAs

remains open (Fig. 6E). In addition to mRNAs, SGs contain translation-initiation factors, including small ribosome subunits. Thus, our results further suggest that the pool of translation factors sequestered at SGs either represents a minor proportion or a discrete population of inactive molecules. Yet, it should not be ruled out that translation factors and mRNAs transit SGs briefly, and spend most of their time in the cytosol, as reported recently by Mollet et al. (Mollet et al., 2008) for specific reporter molecules. In summary, our results indicate that the delivery of mRNPs to and from silencing foci occurs without major consequences on global protein translation. The effect of SGs on the stability and translation of specific mRNAs, including those encoding stress-induced proteins, remains to be investigated.

The self-assembly of SGs and PBs depends on an equilibrium between actively translating polysomes and silenced mRNPs (reviewed by Anderson and Kedersha, 2008; Franks and Lykke Andersen, 2008). We propose that a balance between anterograde and retrograde motor-driven transport of silenced mRNPs ultimately regulates silencing-foci assembly. Whether cellular stress regulates molecular motor activity or their recruitment to mRNPs is unknown. Several dynein and kinesin subunits as well as adaptor molecules are regulated at distinct levels by specific

stress-induced kinases (Morfini et al., 2001; Fumoto et al., 2006) whose relevance in SG formation and PB growth is not known. The present work has identified motor subunits and adaptor molecules involved in PB and SG induction upon stress, thus establishing a groundwork for future research on the regulation of silencing-foci dynamics.

Materials and Methods

Cell culture, stress induction, immunofluorescence and western blot

NIH3T3 and COS-7 cells from the American Type Culture Collection (ATCC) were grown in DMEM or MEM (Sigma) supplemented with 10% fetal bovine serum (Natocor, Córdoba, Argentina), penicillin and streptomycin (Sigma). Schneider S2R+ cells from the *Drosophila* Genomic Resource Center (Indiana University, Bloomington, IN) were grown in M3 + BYPE supplemented as above. The following drugs from Sigma were added to conditioned media and used as follows, unless otherwise indicated: thapsigargin, 100 nM; sodium arsenite, 0.25 mM; cycloheximide, and puromycin, 0.1 mg/ml. Cytochalasin B (50 µg/ml) and colchicine (10 µM) (Sigma) were added over 1 hour at 37°C to the culture medium prior to stress induction. Immunofluorescence was performed after fixation, permeabilization and blocking as usual, unless otherwise indicated, or after treatment of live cells in 0.1% Triton X-100 (Fig. 1A-C, Fig. 3A-D and supplementary material S2C-E), as previously done (Thomas et al., 2005). Primary antibodies were diluted as follows: rabbit polyclonal antibodies against Giantin, 1:1000; KIF5B, directed against aa 376-396, 1:100, both from Abcam (Cambridge, UK); RLS1 anti-Staufen-1 (Thomas et al., 2005), 1:500; anti-PABP (kindly provided by Evita Mohr, University of Hamburg, Germany), 1:500; anti-Dcp1 (generous gift from Jens Lykke Andersen, University of Colorado, CO), 1:500; anti-MnSOD, 1:200; anti-phospho-eIF2α, 1:100, both from Stressgen (Victoria, British Columbia, Canada); anti-Myc-Tag (Cell Signaling Technology, Danvers, MA) 1:100; anti-DHC (Santa Cruz Biotechnology, Santa Cruz, CA), 1:50; anti-DIC (Chemicon International, Temecula, CA), 1:50; goat polyclonal anti-TIA-1 (Santa Cruz), 1:100; and anti-eIF3η (Santa Cruz), 1:200. Monoclonal antibodies anti-γ-tubulin (SIGMA); 1:10,000, anti-β-tubulin (SIGMA), 1:500; anti-TIAR (BD Biosciences, San José, CA); anti-PDI (Stressgen), 1:100; anti-KHC clones H1, directed against the N-terminus, and H2, directed against aa 400-600 of mammalian KIF5A, KIF5B and KIF5C (DeBoer et al., 2008), 1:50, both from Chemicon; anti-KLC clones L1, directed against the N-terminus of KLC1 and KLC2, and L2, directed against the C-terminal of mouse KLC1 (DeBoer et al., 2008), 1:50 (generous gift from Gerardo Morfini, University of Illinois at Chicago, IL). Secondary antibodies were from Molecular Probes (Invitrogen, Carlsbad, CA) or Jackson ImmunoResearch Laboratories (West Grove, PA). FITC-conjugated phalloidin was from SIGMA, 1:50. Fluorescent in situ hybridization (FISH) of polyadenylated RNA was performed using a Cy3-labelled oligodT probe (SIGMA) following standard procedures. Cells were mounted in Mowiol 4-88 (Calbiochem, EMD Biosciences, San Diego, CA).

Images were acquired in a PASCAL-LSM and a LSM510 Meta confocal microscopes (Carl Zeiss, Oberkochen, Germany), using C-Apochromat 40×/1.2 W Corr and 63×/1.2 W Corr water-immersion objectives for the LSM, and a EC 'Plan-Neofluor' 40×/1.30 Oil and Plan-Apochromat 63×/1.4 Oil for the LSM510 Meta. Images were acquired with Zeiss LSM software at 25°C. Equipment adjustment was assessed using 1 µm FocalCheck fluorescent microspheres (Molecular Probes).

Western blotting from post-nuclear cell extracts was performed by standard procedures using LumiGlo (Cell Signaling) and Hyperfilm (Amersham Biosciences). Primary antibodies were used as follows: monoclonal anti-KHC clone H2, 1:500; anti-β actin (SIGMA), 1:1000; anti-SUK4 (DSHB, Iowa, IA); anti-KLC clone 63/90 (DeBoer et al., 2008), 1:500; anti-tyrosine tubulin, clone TUB-1A2 (SIGMA), 1:20,000; and anti-phospho-eIF2α, 1:1000. Autoradiographs were scanned and signal intensity assessed with ImageJ (NIH) software.

siRNA treatment

Two sets of siRNA against mouse *DHC1* and *DHC2*, siDHC1 and siDHC2, respectively, were used. Set 'A', from Ambion (Austin, TX): 5′-GAAGGT-CATGAGCCAAGAA-3′ against *DHC1*, and pre-designed siRNA 194763 and 194762 against DHC2 were used in Fig. 1 and supplementary material Fig. S3A,B. Set 'B', from Dharmacon (Chicago, IL), containing pools of four sequences, L-058788-00 against *DHC1* and L-061741-00 against *DHC2* was used in Figs 3, 4 and supplementary material Fig. S3C. Dharmacon pool siRNAs L-040710-01, L-042990-01, L-058772-01, L-046959-01, L-046961-01 and L-059477-01 against all described splicing variants of murine *KIF5B*, *BicD1*, *BicD2*, *KLC1*, *KLC2* and protein interacting with APP tail 1 (PAT1), respectively; D-001810-10 siCONTROL non-targeting pool (siNTpool) and a non-targeting siRNA (siNT) 5′-UAGCGA-CUAAACACAUCAAUU-3′ were used. Mammalian cells were treated with TransIT-TKO (Dharmacon) and 100 nM siRNAs unless otherwise indicated, and analyzed 72 hours later. When two genes were simultaneously targeted, 50 nM of each siRNA was used. dsRNA for use in S2R+ cells was prepared by in vitro transcription of the following amplicons from the *Drosophila* RNAi Screening Center (Harvard Medical School, Boston, MA): DRSC08656 for *DHC64C* and DRSC07448 for *KHC*. S2R+

cells were plated with 5 µg of the corresponding dsRNA using serum-free media, and 10% FBS was added after 1 hour. A booster with 5 µg of siRNA was performed 3 days later, and cells were analyzed 2 days afterwards.

Protein-synthesis assay

A custom-made L-amino-acid mixture [^{14}C(U)] containing alanine, arginine, glutamic acid, lysine and serine (Perkin Elmer, Boston, MA) was added to cells plated in 10-mm wells during 30 minutes. At the indicated times, the supernatant was removed, cells where washed in PBS and lysed in RIPA buffer. Trichloroacetic-acid-insoluble radioactivity relative to total radioactivity in the lysates was evaluated in duplicate measurements of triplicate wells for each point.

Statistics

Unless otherwise indicated, SGs were identified by TIAR staining as described (Thomas et al., 2009), and cells were scored as positives with at least three foci of a minimal size of 0.5 µm, because cells with less than five SGs were infrequent in all tested conditions, and SGs are usually 0.5-10 µm in size. Approximately 150 cells for each time-point from duplicate coverslips were analyzed. PBs were analyzed in at least 20 randomly selected cells from duplicate coverslips. P-values (*$P<0.05$; **$P<0.01$; ***$P<0.001$) relative to control treatments according to two-way ANOVA or the indicated test were determined using Infostat (Universidad Nacional de Córdoba, Argentina) or Instat (GraphPad Software, San Diego, CA) software.

References

Aizer, A., Brody, Y., Ler, L. W., Sonenberg, N., Singer, R. H. and Shav-Tal, Y. (2008). The dynamics of mammalian P body transport, assembly, and disassembly in vivo. *Mol. Biol. Cell* **19**, 4154-4166.

Anderson, P. and Kedersha, N. (2006). RNA granules. *J. Cell Biol.* **172**, 803-808.

Anderson, P. and Kedersha, N. (2008). Stress granules: the Tao of RNA triage. *Trends Biochem. Sci.* **33**, 141-150.

Arimoto, K., Fukuda, H., Imajoh-Ohmi, S., Saito, H. and Takekawa, M. (2008). Formation of stress granules inhibits apoptosis by suppressing stress-responsive MAPK pathways. *Nat. Cell Biol.* **10**, 1324-1332.

Buchan, J. R., Muhlrad, D. and Parker, R. (2008). P bodies promote stress granule assembly in *Sacharomyces cerevisiae*. *J. Cell Biol.* **183**, 441-455.

Brengues, M., Teixeira, D. and Parker, R. (2005). Movement of eukaryotic mRNAs between polysomes and cytoplasmic processing bodies. *Science* **310**, 486-489.

Bullock, S. L., Nicol, A., Gross, S. P. and Zicha, D. (2006). Guidance of bidirectional motor complexes by mRNA cargoes through control of dynein number and activity. *Curr. Biol.* **16**, 1447-1452.

Burakov, A., Kovalenko, O., Semenova, I., Zhapparova, O., Nadezhdina, E. and Rodionov, V. (2008). Cytoplasmic dynein is involved in the retention of microtubules at the centrosome in interphase cells. *Traffic.* **9**, 472-480.

Deacon, S. W., Serpinskaya, A. S., Vaughan, P. S., Lopez Fanarraga, M., Vernos, I., Vaughan, K. T. and Gelfand, V. I. (2003). Dynactin is required for bidirectional organelle transport *J. Cell Biol.* **160**, 297-301.

DeBoer, S. R., You, Y., Szodorai, A., Kaminska, A., Pigino, G., Nwabuisi, E., Wang, B., Estrada-Hernandez, T., Kins, S., Brady, S. T. et al. (2008). Conventional kinesin holoenzymes are composed of heavy and light chain homodimers. *Biochemistry* **47**, 4535-4543.

Delanoue, R., Herpers, B., Soetaert, J., Davis, I. and Rabouille, C. (2007). *Drosophila* Squid/hnRNP helps dynein switch from a gurken mRNA transport motor to an ultrastructural static anchor in sponge bodies. *Dev. Cell* **13**, 523-538.

Dictenberg, J. B., Swanger, S. A., Antar, L. N., Singer, R. H. and Bassell, G. J. (2008). A direct role for FMRP in activity-dependent dendritic mRNA transport links filopodial-spine morphogenesis to fragile X syndrome. *Dev. Cell.* **14**, 926-939.

Eisinger-Mathason, T. S., Andrade, J., Groehler, A. L., Clark, D. E., Muratore-Schroeder, T. L., Pasic, L., Smith, J. A., Shabanowitz, J., Hunt, D. F., Macara, I. G. et al. (2008). Codependent functions of RSK2 and the apoptosis-promoting factor TIA-1 in stress granule assembly and cell survival. *Mol. Cell* **31**, 722-736.

Eulalio, A., Behm-Ansmant, I. and Izaurralde, E. (2007a). P bodies: at the crossroads of post-transcriptional pathways *Nat. Rev Mol. Cell. Biol.* **8**, 9-22.

Eulalio, A., Behm-Ansmant, I., Schweizer, D. and Izaurralde, E. (2007b). P-body formation is a consequence, not the cause, of RNA-mediated gene silencing. *Mol. Cell. Biol.* **27**, 3970-3981.

Fenger-Grøn, M., Fillman, C., Norrild, B. and Lykke-Andersen, J. (2005). Multiple processing body factors and the ARE binding protein TTP activate mRNA decapping. *Mol. Cell.* **20**, 905-915.

Franks, T. M. and Lykke-Andersen, J. (2008). The control of mRNA decapping and P-body formation. *Mol. Cell.* **32**, 605-615.

Fumoto, K., Hoogenraad, C. C. and Kikuchi, A. (2006). GSK-3beta-regulated interaction of BICD with dynein is involved in microtubule anchorage at centrosome. *EMBO J.* **25**, 5670-5682.

Hoogenraad, C. C., Akhmanova, A., Howell, S. A., Dortland, B. R., De Zeeuw, C. I., Willemsen, R., Visser, P., Grosveld, F. and Galjart, N. (2001). Mammalian Golgi-associated Bicaudal-D2 functions in the dynein-dynactin pathway by interacting with these complexes. *EMBO J.* **20**, 4041-4054.

Horne-Badovinac, S. and Bilder, D. (2008). Dynein regulates epithelial polarity and the apical localization of stardust A mRNA. *PLoS Genet.* **4(1)**, e8.

Hughes, J. R., Bullock, S. L. and Ish-Horowicz, D. (2004). Inscuteable mRNA localization is dynein-dependent and regulates apicobasal polarity and spindle length in Drosophila neuroblasts. *Curr. Biol.* **14**, 1950-1956.

Ivanov, P. A., Chudinova, E. M. and Nadezhdina, E. S. (2003). Disruption of microtubules inhibits cytoplasmic ribonucleoprotein stress granule formation. *Exp. Cell Res.* **290**, 227-233.

Kanai, Y., Dohmae, N. and Hirokawa, N. (2004). Kinesin transports RNA: isolation and characterization of an RNA-transporting granule. *Neuron* **43**, 513-525.

Kedersha, N., Cho, M. R., Li, W., Yacono, P. W., Chen, S., Gilks, N., Golan, D. E. and Anderson, P. (2000). Dynamic shuttling of TIA-1 accompanies the recruitment of mRNA to mammalian stress granules. *J. Cell Biol.* **151**, 1257-1268.

Kedersha, N., Stoecklin, G., Ayodele, M., Yacono, P., Lykke-Andersen, J., Fritzler, M. J., Scheuner, D., Kaufman, R. J., Golan, D. E. and Anderson, P. (2005). Stress granules and processing bodies are dynamically linked sites of mRNP remodeling. *J. Cell Biol.* **169**, 871-884.

Kim, W. J., Kim, J. H. and Jang, S. K. (2007). Anti-inflammatory lipid mediator 15d-PGJ2 inhibits translation through inactivation of eIF4A. *EMBO J.* **26**, 5020-5032.

Kolobova, E., Efimov, A., Kaverina, I., Rishi, A. K., Schrader, J. W., Ham, A. J., Larocca, M. C. and Goldenring, J. R. (2009). Microtubule-dependent association of AKAP350A and CCAR1 with RNA stress granules. *Exp. Cell Res.* **315**, 542-555.

Kopito, R. R. (2000). Aggresomes, inclusion bodies and protein aggregation. *Trends Cell Biol.* **10**, 524-530.

Kwon, S., Zhang, Y. and Matthias, P. (2007). The deacetylase HDAC6 is a novel critical component of stress granules involved in the stress response. *Genes Dev.* **21**, 3381-3394.

Leung, A. K., Calabrese, J. M. and Sharp, P. A. (2006). Quantitative analysis of Argonaute protein reveals microRNA-dependent localisation to stress granules. *Proc. Natl. Acad. Sci. USA* **103**, 18125-18130.

Li, Z., Wang, L., Hays, T. S. and Cai, Y. (2008). Dynein-mediated apical localization of crumbs transcripts is required for Crumbs activity in epithelial polarity. *J. Cell Biol.* **180**, 31-38.

Lin, J. C., Hsu, M. and Tarn, W. Y. (2007). Cell stress modulates the function of splicing regulatory protein RBM4 in translation control. *Proc. Natl. Acad. Sci. USA* **104**, 2235-2240.

Ling, S. C., Fahrner, P. S., Greenough, W. T. and Gelfand, V. I. (2004). Transport of *Drosophila* fragile X mental retardation protein-containing ribonucleoprotein granules by kinesin-1 and cytoplasmic dynein. *Proc. Natl. Acad. Sci. USA* **101**, 17428-17433.

Matanis, T., Akhmanova, A., Wulf, P., Del Nery, E., Weide, T., Stepanova, T., Galjart, N., Grosveld, F., Goud, B., De Zeeuw, C. I. et al. (2002). Bicaudal-D regulates COPI-independent Golgi-ER transport by recruiting the dynein-dynactin motor complex. *Nat. Cell Biol.* **4**, 986-992.

Mazan-Mamczarz, K., Lal, A., Martindale, J. L., Kawai, T. and Gorospe, M. (2006). Translational repression by RNA-binding protein TIAR. *Mol. Cell. Biol.* **26**, 2716-2727.

Mazroui, R., Di Marco, S., Kaufman, R. J. and Gallouzi, I. E. (2007). Inhibition of the ubiquitin-proteasome system induces stress granule formation. *Mol. Biol. Cell* **18**, 2603-2618.

Mollet, S., Cougot, N., Wilczynska, A., Dautry, F., Kress, M., Bertrand, E. and Weil, D. (2008). Translationally repressed mRNA transiently cycles through stress granules during stress. *Mol. Biol. Cell* **19**, 4469-4479.

Morfini, G., Szebenyi, G., Richards, B. and Brady, S. T. (2001). Regulation of kinesin: implications for neuronal development. *Dev. Neurosci.* **23**, 364-376.

Ohn, T., Kedersha, N., Hickman, T., Tisdale, S. and Anderson, P. (2008). A functional RNAi screen links O-GlcNAc modification of ribosomal proteins to stress granule and processing body assembly. *Nat. Cell Biol.* **10**, 1224-1231.

Palacios, I. M. and St Johnston, D. (2002). Kinesin light chain-independent function of the Kinesin heavy chain in cytoplasmic streaming and posterior localisation in the *Drosophila* oocyte. *Development* **129**, 5473-5485.

Parker, R. and Sheth, U. (2007). P Bodies and the control of mRNA translation and degradation. *Mol. Cell* **25**, 635-646.

Scadden, A. D. (2007). Inosine-containing dsRNA binds a stress-granule-like complex and downregulates gene expression in trans. *Mol. Cell.* **28**, 491-500.

Sivan, G., Kedersha, N. and Elroy-Stein, O. (2007). Ribosomal slowdown mediates translational arrest during cellular division. *Mol. Cell. Biol.* **27**, 6639-6646.

Stöhr, N., Lederer, M., Reinke, C., Meyer, S., Hatzfeld, M., Singer, R. H. and Hüttelmaier, S. (2006). ZBP1 regulates mRNA stability during cellular stress. *J. Cell Biol.* **175**, 527-534.

Tanaka, Y., Kanai, Y., Okada, Y., Nonaka, S., Takeda, S., Harada, A. and Hirokawa, N. (1998). Targeted disruption of mouse conventional kinesin heavy chain, Kif5B, results in abnormal perinuclear clustering of mitochondria. *Cell* **93**, 1147-1158.

Thomas, M. G., Martinez Tosar, L. J., Loschi, M., Pasquini, J. M., Correale, J., Kindler, S. and Boccaccio, G. L. (2005). Staufen recruitment into stress granules does not affect early mRNA transport in oligodendrocytes. *Mol. Biol. Cell* **16**, 405-420.

Thomas, M. G., Martinez Tosar, L. J., Desbats, M. A., Leishman, C. C. and Boccaccio, G. L. (2009). Mammalian Staufen 1 is recruited to stress granules and impairs their assembly. *J. Cell Sci.* **122**, 563-573.

Tourrière, H., Chebli, K., Zekri, L., Courselaud, B., Blanchard, J. M., Bertrand, E. and Tazi, J. (2003). The RasGAP-associated endoribonuclease G3BP assembles stress granules. *J. Cell Biol.* **160**, 823-831.

Tsai, N. P., Ho, P. C. and Wei, L. N. (2008). Regulation of stress granule dynamics by Grb7 and FAK signaling pathway. *EMBO J.* **27**, 715-726.

Tsai, N. P., Tsui, Y. C. and Wei, L. N. (2009). Dynein motor contributes to stress granule dynamics in primary neurons. *Neuroscience* **159**, 647-656.

Yu, C., York, B., Wang, S., Feng, Q., Xu, J. and O'Malley, B. W. (2007). An essential function of the SRC-3 coactivator in suppression of cytokine mRNA translation and inflammatory response. *Mol. Cell* **25**, 765-778.

Journal of Cell Science